

Deep learning algorithm for CT scanning in ankle trauma: Technical principles and prospects for reducing effective radiation dose

M. Zhang¹, M. Lei¹, F. Lin¹, Y. Chen¹, Y. Xie¹, J. Liu¹, J. Chen¹, H. Wang², M. Xiao^{1*}

¹Department of Radiology, Zhuhai Hospital, Guangdong Provincial Hospital of Traditional Chinese Medicine, 53 Jingle Road, Zhuhai City, Guangdong Province, China

²Guizhou Medical University, Grade 2022 Imaging medicine major, Gouzhou City, Gouzhou Province, China

ABSTRACT

► Short report

*Corresponding author:

Mengqiang Xiao, M.D.

E-mail: xmqzhuhai@163.com

Received: January 2023

Final revised: June 2024

Accepted: August 2024

Int. J. Radiat. Res., July 2025;
23(3): 813-817

DOI: 10.61186/ijrr.23.3.39

Keywords: Deep learning algorithm, ankle fracture, computer tomography, low radiation dose.

Background: This study aims to compare the image quality and effective dose (ED) of deep learning algorithm computer tomography (DLA-CT) with standard CT (SD-CT) in managing ankle trauma. **Materials and Methods:** In this prospective study, 88 patients underwent random allocation to either the SD-CT group (utilizing a tube voltage of 120KV and an automatic tube current milliampere setting) or the DLA-CT group (employing automatic tube voltage and current adjustments). Senior radiologists assessed objective image quality using parameters such as noise, signal-to-noise ratio (SNR), and contrast-to-noise ratio (CNR). The influence of subjective image quality and its impact on treatment plans were evaluated using a 5-point Likert scale, with scores of 3 or higher indicating acceptable image quality and adherence to treatment plan requirements. Dose length product (DLP) (mGy×cm) was automatically recorded by the scanner software, DLP×k. **Results:** Objective image quality with DLA-CT was found to be inferior to that obtained with SD-CT ($P < 0.001$). No significant differences were noted in subjective image quality scores between the two groups ($P = 0.60$). Additionally, both subjective image quality scores and the effect of image quality on treatment decisions were scored at 3 or higher. The ED was significantly reduced by 48.83% in the DLA-CT group compared to the SD-CT group ($21.42 \pm 2.62 \mu\text{Sv}$ and $10.96 \pm 1.12 \mu\text{Sv}$, respectively, $P = 0.001$). **Conclusion:** DLA-CT proves effective in the management of ankle trauma, significantly reducing ED while meeting clinical diagnostic and treatment standards.

INTRODUCTION

Ankle fracture is one of the common clinical diseases ⁽¹⁾. Traditional digital radiography (DR) imaging exhibits limited sensitivity in pinpointing joint fractures, thereby falling short in accurately categorizing the fracture type and potentially leading to misdiagnoses ⁽²⁾. In contrast, computer tomography (CT) scans can precisely delineate the characteristics and types of ankle fractures, emerging as the gold standard for diagnosing fractures and facilitating comprehensive treatment planning ⁽³⁾. Accompanying the proliferation of CT machinery, an escalating number of individuals are undergoing CT scans. Data indicates a 300% surge in CT scan administrations in the United States from 1993 to 2007, totaling 71.7 million. Notably, the effective dose (ED) from CT scans constitutes approximately 70% of the total ED from all radiographic examinations, with malignancies attributed to CT radiation doses

representing 0.4% of all cancer cases ⁽⁴⁾. Machine learning, a burgeoning field in contemporary computing, has been the focus of extensive research aimed at enhancing machine intelligence. This discipline regards learning as a pivotal feature, not only intrinsic to human behavior but also as a vital component in machine functionality ⁽⁵⁻⁸⁾. Generally, deep learning algorithms emulate neural networks akin to human brain connections, integrating artificial intelligence within computer systems, thereby augmenting the speed and accuracy of several critical tasks ⁽⁹⁻¹¹⁾.

Currently, numerous hospitals implement fixed tube voltage and current settings for limb scanning procedures ⁽¹²⁾. To mitigate the radiation exposure from CT scans, a protocol involving a 120 kV fixed tube voltage coupled with an automatic tube current has been introduced for clinical osteomuscular examinations ⁽¹³⁾. This method is progressively being embraced for limb scanning practices ⁽¹⁴⁾ and has

garnered widespread application in diagnosing ankle fractures (2). In our institution, the standard computer tomography (SD-CT) procedure for the ankle joint incorporates a 120 kV tube voltage and an automated tube current. Additionally, the Siemens CT equipment is equipped with a deep-learning algorithm computer tomography (DLA-CT) scanning technology specifically designed for lower limb vascular imaging. This protocol intuitively adjusts the tube voltage and current based on the distinctive anatomical sections of the lower limbs being scanned, ranging from the hip joint to the foot. Given that ankle joint scans are an integral component of this protocol. This protocol intuitively adjusts the tube voltage and current based on the distinctive anatomical sections of the lower limbs being scanned, ranging from the hip joint to the foot. Given that ankle joint scans are an integral component of this protocol.

As far as our understanding extends, there exist no accounts concerning the application of DLA-CT for ankle joint scans. The present study endeavored to apply this protocol to patients with ankle joint injuries, aiming to evaluate the image quality and ED of DLA-CT technology in comparison to conventional SD-CT techniques in ankle trauma.

MATERIALS AND METHODS

Patients

This prospective study was approved by the Ethics Committee of Guangdong Provincial Hospital of Chinese Medicine (ZE2023298) in January 20, 2023. A cohort of 88 ankle trauma CT cases, documented at between January 30, 2023, and December 25, 2023, were assembled and arbitrarily segregated into SD-CT and DLA-CT groups, comprising 44 cases each. There were no splints/plaster external fixations in any of the scans.

Inclusion criteria: Individuals aged 18 years and above, presenting a distinct history of trauma and necessitating a preoperative CT scan to formulate treatment strategies, or those suspected of harboring fractures requiring verification.

Exclusion criteria: The study precluded individuals with metal internal fixtures, tumors, arthritis, or underlying conditions conducive to compromised bone metabolism.

Gold Standard for Fracture Identification: Surgical diagnosis or subsequent CT/DR review was deemed as the definitive indicators of fractures (15).

Scan protocols

Imaging protocols were implemented using a multi-slice CT scanner (SOMATOM Drive VA62A, Siemens Healthcare GmbH, Erlangen, Germany). This DLA-CT scanning software was purchased concurrently with the CT unit. The SD-CT scan parameters involved a tube voltage of 120 kV coupled

with an automated milliamperere tube current. Conversely, the DLA-CT adopted an automatic tube voltage (with potential settings of 120 kV, 110 kV, 100 kV, 90 kV, 80 kV) and an automated milliamperere tube current. Both the SD-CT and DLA-CT groups utilized a bone window reconstruction strategy with a scanning length of 200 mm, a field of view (FOV) of 150 mm, a slice thickness of 1 mm, and a 1 mm interval.

Radiation dose

Computed Tomography Dose Index volume (CTDIvol) (mGy) and Dose length product (DLP) (mGy×cm) were automatically indicated by the scanner software for all CT-protocols. $ED = DLP \times k$, $k = 0.0002$ has been used for extremity scans (15).

Fracture interpretation and image evaluation

Two seasoned radiologists, with ten and thirteen years of experience respectively, independently conducted dual assessments of the fractures with a minimum six-week interval between evaluations. Discrepancies between the resultant four analyses were systematically reconciled.

Objective image quality (16): Within the Siemens CT post-processing station (syngo.via), a senior radiologist meticulously selected three distinct layers of muscle tissue surrounding the joint for CT value assessment. The region of interest (ROI) spanned 70 mm², facilitating the acquisition of the mean muscle CT value (CTm) and muscle standard deviation (SDm). The CT value of the thickest part of the three different layers of bone cortex of the joint was measured, ROI = 8 mm², and the mean CT value (CTb) of the three measurements was obtained. Noise = SDm, SNR = CTm / SDm, CNR = CTb / SDm.

Subjective image quality (16): At the Siemens CT post processing station (syngo.via), images were anonymized. The quality of these images was subjectively evaluated by two senior radiologists, while two orthopedic physicians assessed the impact of image quality on the treatment plan. Evaluations were performed using a double-blind 5-point Likert scale (5=excellent; 4=good; 3=qualified; 2=poor; 1=very poor; 3 was the chosen cutoff quality, figure 1).



Figure 1. A 5-point Likert-type scale was utilized to assess the subjective quality of CT images and to gauge the influence of this subjective image quality on clinical decision-making related to fractures (indicated by the red arrow) A 3, Qualified; B 4, Good; C 5, Excellent.

Statistical analysis

The statistical analysis was executed utilizing the SPSS software, version 27.0 (IBM Corp, Armonk, NY, USA). Gender differences and diagnostic fracture effects between the groups were ascertained using the kappa test. The ANOVA test facilitated the analysis of homogenous variances of measurement data, encompassing parameters like age, CTDIvol, DLP, ED, noise, SNR, and CNR. In instances of non-homogeneous variances, Tamhane's T2 test was employed, establishing $P < 0.05$ as the threshold for statistical significance. The Chi-square test was employed to assess CT image subjective scores and the influence of image quality on treatment plan scores. Consistency across subjective scores and image quality evaluations by the two physicians was gauged using the Intra-class Correlation Coefficient (ICC) test, which delineated consistency levels as follows: < 0.40 : poor consistency; $0.41 \sim 0.60$: medium consistency; $0.61 \sim 0.80$: good agreement;

$0.81 \sim 1.00$: perfect consistency.

RESULTS

The SD-CT group consisted of 20 males and 24 females, compared to 19 males and 25 females in the DLA-CT group, a difference that was not statistically significant ($P=0.83$). Moreover, there was no notable disparity in the average age between the groups (table 1). The breakdown of diagnoses was as follows: 34 fractures and 10 normal cases in the SD-CT group, and 35 fractures and 9 normal cases in the DLA-CT group, with no missed diagnoses or misdiagnoses in either the DLA-CT or SD-CT groups, with no significant difference in the sensitivity, specificity, and diagnostic accuracy between the groups ($P=0.99$). The ED observed in the SD-CT group was notably higher than that in the DLA-CT group ($P<0.001$).

Table 1. Age, image quality, and radiation dose with standard CT and deep Learning Algorithm CT.

Group, n	Age (year)	Noise	SNR	CNR	CTDIvol (mGy)	DLP (mGy•cm)	ED (μSv)	Image Clarity scoring	Clinical Decision-making scoring
SD-CT 44 44	44.36±17.35	3.69±0.85	17.26±4.26	473.82±117.17	5.89±0.14	107.11±13.09	21.42±2.62	4.55±0.59	5.00±0.00
DLA-CT 44	41.91±14.50	5.40±2.53	13.08±3.69	375.08±106.99	3.05±0.08	54.78±5.58	10.96±1.12	4.61±0.62	5.00±0.00
F-value	0.53	18.02	24.16	17.04	14225.98	594.89	594.89	0.28	0.001
P-value	0.47	<0.001	<0.001	<0.001	<0.001	<0.001	<0.001	0.60	0.99

Image Clarity scoring: SD-CT and ULA-CT, both ICC=0.77; Clinical Decision-making scoring: SD-CT and ULA-CT, both ICC=0.99.

CT: Computed Tomography; N: number of cases; SD-CT: standard CT; DLA-CT: Deep Learning AlgorithmCT; SNR: signal-to-noise ratio; CNR: contrast signal-to-noise ratio; CTDIvol: the volume CT dose index; DLP: dose-length product; ED: effective dose; ICC: Intraclass correlation coefficient.

The objective image quality (including aspects such as noise, SNR, CNR) in the SD-CT scans surpassed that of the DLA-CT scans ($P<0.001$). There was no discernible difference between the SD-CT and DLA-CT groups in terms of subjective image quality and the influence of image quality on the treatment plan ($P=0.60$), with scores consistently being equal to or exceeding 3 points (figures 1-3 and table 1). Noteworthy consistency was observed between the two groups in the subjective evaluations of CT image quality and the effects of image quality on the treatment plan (ICC=0.77, 0.77, 0.99, 99; table 1).

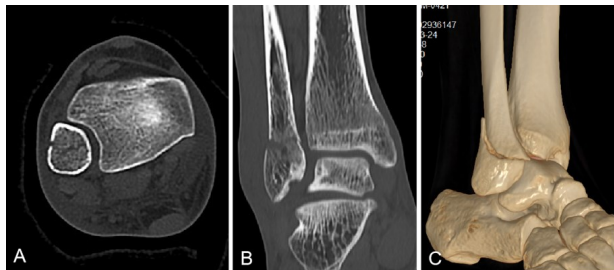


Figure 2. SD-CT, A 42-year-old man patient was diagnosed with Lateral malleolar fractures, **A**, axis position; **B**, Coronal position; **C**, Three-dimensional reconstruction. A, B and C subjective quality 5, Excellent. Noise=3.50, SNR:18.88, CNR:48.51, ED:21.40 μSv.

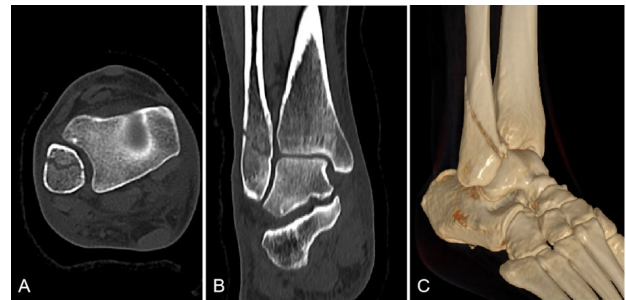


Figure 3. DLA-CT, A 57-year-old female patient was diagnosed with Lateral malleolar fractures, **A** axis position, **B** Coronal position, **C** Three-dimensional reconstruction. A, B and C subjective quality 5, Excellent. Noise:4.03, SNR:15.80; NR:462.83, ED:11.92 μSv.

DISCUSSION

This study contrasted the diagnostic efficacy of DLA-CT and SD-CT in identifying ankle fractures. Results indicated that the ED for the DLA-CT protocol was notably lower than that of the SD-CT. While the image quality of DLA-CT was inferior to SD-CT, the sensitivity, specificity, and diagnostic accuracy of both methods for detecting ankle fractures remained comparable. To our knowledge, this represents the

inaugural study affirming the viability of DLA-CT as a suitable alternative to SD-CT for imaging such fractures.

Adhering to the ALARA (As Low As Reasonably Achievable) principle in radiation safety, an increasing number of scholars have explored the potential of low-dose CT scans for fracture diagnosis in recent years (16-20). Efforts to minimize the ED in CT scans have led to the emergence of various scanning techniques, including personalized CT scanning (21), variable pitch CT scanning (22), and automatic tube current modulation (ATCM) (23). Tube current modulation relies entirely on the positioning image, which embodies the X-ray attenuation attributes of the subject-factors like size, shape, and density. Based on these features, ATCM technology autonomously adjusts the tube current during scanning. Recent advancements in computer technology have ushered in widespread clinical adoption of deep learning algorithms for disease diagnosis (24). These algorithms scanning technology not only enhance the image quality of low-dose CT scans (25) but also mitigate the reliance on technician experience, eliminating concerns over varying scan parameters due to individual patient differences. Concurrently, they significantly diminish the radiation dose associated with CT scans (26). Recent studies have highlighted that utilizing lower tube voltage in CT scans can enhance the contrast between adjacent tissues with varying densities, notably in regions where there is a significant disparity in density, such as between bones and muscles or between enhanced blood vessels and surrounding soft tissues (27, 28). However, it is also noted that while low-dose CT scans do enhance tissue contrast, an overly reduced tube voltage can compromise X-ray penetration and overall image quality (29). Consequently, it is advisable to adjust the tube voltage judiciously based on the specific scanning sites and individual patient characteristics. In recent developments, DLA-CT scanning technology has emerged as a significant advancement. This technique optimally adjusts the tube voltage according to individual patients and scanning sites, and when integrated with ATCM technology, can considerably decrease radiation exposure (30, 31). At present, DLA-CT is extensively utilized in pediatric cases (30) and within the realm of cardiovascular system studies (31). This research delineates the advantages of DLA-CT scanning technology in comparison to ATCM technology.

To the best of our knowledge, there is no documented research addressing the use of DLA-CT scanning within the context of the musculoskeletal system. In this study, we employed DLA-CT scanning technology to conduct CT scans on patients suffering from ankle trauma, revealing a significant 48.83% reduction in the ED as compared to SD-CT scans.

However, this study is not without limitations.

Firstly, DLA-CT scanning technology was fundamentally developed for lower limb blood vessel CT scans, rather than specifically for ankle joint trauma. Its application in this study was thus confined to patients with ankle injuries. Secondly, while the study evaluates the subjective assessment of DLA-CT image quality on treatment planning, it does not investigate any potential differences between SD-CT and DLA-CT scanning methods regarding the intra-operative and postoperative outcomes of fractures.

CONCLUSION

DLA-CT scanning proves to be a viable option for patients with clinically suspected ankle fractures resulting from trauma. When compared to SD-CT, DLA-CT scanning substantially reduces radiation dose, albeit with a slight decrease in objective image quality. However, the subjective image quality remains comparable, satisfactorily meeting the requirements of clinical diagnosis and treatment planning.

ACKNOWLEDGEMENTS

We extend our gratitude to Rulin Xu from Canon Medical Systems (China) Co., LTD for his invaluable contributions to this study.

Funding: No.

Conflicts of interests: The authors affirm that there are no competing interests.

Ethics approval and consent to participate: (1) All study methods were conducted following applicable guidelines and regulations. (2) The experimental protocols received approval and were consented to by the Ethics Committee of Guangdong Provincial Hospital of Traditional Chinese Medicine (ZE2023-298).

Authors' contributions: M Z contributed to drafting the manuscript. M L, FH L, YZ X, and H W participated in data collection and figure preparation. FJ L was responsible for designing the manuscript. J C and MQ X engaged in data analysis and interpretation. In the final stages, M Zhang, YX C, and MQ X critically reviewed and revised the manuscript.

REFERENCES

1. Martijn HA, Lambers KTA, Dahmen J, *et al.* (2021) High incidence of (osteo)chondral lesions in ankle fractures. *Knee Surg Sports Traumatol Arthrosc*, **29**(5): 1523-1534.
2. Xue P, Chen X, Chen S, *et al.* (2021) The value of CT 3D reconstruction in the classification and nursing effect evaluation of ankle fracture. *J Healthc Eng*, **2021**: 9596518.
3. Cuddy K, Khatib B, Bell RB, *et al.* (2018) Use of intraoperative computed tomography in craniomaxillofacial trauma surgery. *J Oral Maxillofac Surg*, **76**(5): 1016-1025.
4. Azman RR, Shah MNM, Ng KH (2019) Radiation safety in emergency medicine: Balancing the benefits and risks. *Korean J Radiol*, **20**(3): 399-404.

5. Shinde PP and Shah S (2018) A review of machine learning and deep learning applications[C]//2018 Fourth international conference on computing communication control and automation (ICCUBEA). *IEEE*, **4**: 1-6.
6. Handelman GS, Kok HK, Chandra RV, et al. (2018) eDoctor: machine learning and the future of medicine. *Journal of Internal Medicine*, **284**(6): 603-619.
7. Lee YW, Choi JW, Shin EH (2021) Machine learning model for predicting malaria using clinical information. *Computers in Biology and Medicine*, **129**: 104151.
8. Sultan AS, Elgharib MA, Tavares T, et al. (2020) The use of artificial intelligence, machine learning and deep learning in oncologic histopathology. *J Oral Pathol Med*, **49**(9): 849-856.
9. Ranganathan DG (2021). A study to find facts behind preprocessing on deep learning algorithms. *Journal of Innovative Image Processing*, **3**(1): 66-74.
10. Oh JH, Kim HG, Lee KM (2023) Developing and evaluating deep learning algorithms for object detection: key points for achieving superior model performance. *Korean Journal of Radiology*, **24**(7): 698-714.
11. Achuthan S, Chatterjee R, Kotnala S, et al. (2022) Leveraging deep learning algorithms for synthetic data generation to design and analyze biological networks. *J Biosci*, **47**: 43.
12. Zhang M, Lei M, Zhang J, et al. (2022) Feasibility study of three-dimensional printing knee model using the ultra-low-dose CT scan for preoperative planning and simulated surgery. *Insights Imaging*, **13**(1): 151.
13. Lei M, Zhang M, Luo N, et al. (2022) The clinical performance of ultra-low-dose shoulder CT scans: The assessment on image and physical 3D printing models. *PLoS One*, **17**(9): e0275297.
14. Weinrich JM, Well L, Regier M, et al. (2018) MDCT in suspected lumbar spine fracture: comparison of standard and reduced dose settings using iterative reconstruction. *Clin Radiol*, **73**(7): 675.e9-675.e15.
15. Lei M, Zhang M, Li H, et al. (2022) The diagnostic performance of ultra-low-dose 320-row detector CT with different reconstruction algorithms on limb joint fractures in the emergency department. *Jpn J Radiol*, **40**(10): 1079-1086.
16. Xiao M, Zhang M, Lei M, et al. (2023) Diagnostic accuracy of ultra-low-dose CT compared to standard-dose CT for identification of non-displaced fractures of the shoulder, knee, ankle, and wrist. *Insights Imaging*, **14**(1): 40.
17. Jin L, Ge X, Lu F, et al. (2018) Low-dose CT examination for rib fracture evaluation: A pilot study. *Medicine*, **97**(30): e11624.
18. Murphy MC, Gibney B, Walsh J, et al. (2022) Ultra-low-dose cone-beam CT compared to standard dose in the assessment for acute fractures. *Skeletal Radiology*, **51**(1): 153-159.
19. Alagic Z, Bujila R, Enocson A, et al. (2020) Ultra-low-dose CT for extremities in an acute setting: initial experience with 203 subjects. *Skeletal radiology*, **49**(4): 531-539.
20. Elegbede A, Diaconu S, Dreizin D, et al. (2020) Low-dose computed tomographic scans for postoperative evaluation of craniomaxillofacial fractures: A pilot clinical study. *Plastic and Reconstructive Surgery*, **146**(2): 366-370.
21. Goetti R, Leschka S, Desbiolles L, et al. (2010) Quantitative computed tomography liver perfusion imaging using dynamic spiral scanning with variable pitch: feasibility and initial results in patients with cancer metastases. *Invest Radiol*, **45**(7): 419-26.
22. Tang S, Zhang G, Chen Z, et al. (2021) Application of prospective ECG-gated multiphase scanning for coronary CT in children with different heart rates. *Jpn J Radiol*, **39**(10): 946-955.
23. Yang Z and Liu Z (2020) The efficacy of 18F-FDG PET/CT-based diagnostic model in the diagnosis of colorectal cancer regional lymph node metastasis. *Saudi J Biol Sci*, **27**(3): 805-811.
24. Wang X, Zhang J, Yang S, et al. (2023) A generalizable and robust deep learning algorithm for mitosis detection in multicenter breast histopathological images. *Med Image Anal*, **84**: 102703.
25. Sakai Y, Hida T, Matsuura Y, et al. (2023) Impact of a new deep-learning-based reconstruction algorithm on image quality in ultra-high-resolution CT: clinical observational and phantom studies. *Br J Radiol*, **96**(1141): 20220731.
26. Lee KH, Lee JM, Moon SK, et al. (2012) Attenuation-based automatic tube voltage selection and tube current modulation for dose reduction at contrast-enhanced liver CT. *Radiology*, **265**(2): 437-47.
27. Lv P, Zhou Z, Liu J, et al. (2019) Can virtual monochromatic images from dual-energy CT replace low-kVp images for abdominal contrast-enhanced CT in small- and medium-sized patients? *Eur Radiol*, **29**(6): 2878-2889.
28. Gokalp G (2019) Low kilovolt" prospective ECG-triggering" vs." retrospective ECG-gating" coronary CTA: comparison of image quality and radiation dose. *International Journal of Radiation Research*, **17**(2): 209-216.
29. Xiao M, Zhang M, Liu J, et al. (2017) Iterative reconstruction combined with low dose CT in diagnosis of lumbar intervertebral disc hernia. *Chinese Journal of Medical Imaging Technology*, **33**(3): 458-461.
30. Papadakis AE and Damilakis J (2019) Automatic tube current modulation and tube voltage selection in pediatric computed tomography: A phantom study on radiation dose and image quality. *Invest Radiol*, **54**(5): 265-272.
31. Euler A, Taslimi T, Eberhard M, et al. (2021) Computed tomography angiography of the aorta-optimization of automatic tube voltage selection settings to reduce radiation dose or contrast medium in a prospective randomized trial. *Invest Radiol*, **56**(5): 283-291.

